Physics and Chemistry of the Earth 85–86 (2015) 141–149

Contents lists available at ScienceDirect

Physics and Chemistry of the Earth

journal homepage: www.elsevier.com/locate/pce

# VLF/LF signal studies of the ionospheric response to strong seismic activity in the Far Eastern region combining the DEMETER and ground-based observations

A. Rozhnoi [a,*], M. Solovieva [a], M. Parrot [b], M. Hayakawa [c], P.-F. Biagi [d], K. Schwingenschuh [e], V. Fedun [f]

[a] Institute of the Earth Physics, RAS, Moscow, Russia
[b] LPC2E/CNRS Orleans, France
[c] University of Electro-Communications, Chofu, Tokyo, Japan
[d] Department of Physics, University of Bari, Bari, Italy
[e] Space Research Institute, Austrian Academy of Sciences, Graz, Austria
[f] University of Sheffield, Sheffield, UK

ARTICLE INFO

*Article history:*
Received 20 October 2014
Received in revised form 1 February 2015
Accepted 6 February 2015
Available online 21 February 2015

*Keywords:*
Electromagnetic signals
The ionosphere
Satellite observations
Earthquake precursors

ABSTRACT

The paper presents the results of a joint analysis of ground-based and satellite observations of very low-frequency and low-frequency (VLF/LF) signals during periods of strong seismic activity in the region of Kuril Islands and Japan in 2004–2010. Ground and satellite data was processed using a method based on the difference between the real signal in nighttime and that of a model. The results of the analysis show a good correlation between ground-based and satellite data for several cases of strong ($M \geqslant 6.8$) earthquakes.



## 1. Introduction

French micro-satellite DEMETER had a low-altitude (~710 km) and a nearly polar orbit (Cussac et al., 2006). The launch by CNES (French National Space Agency) was in June 2004, and the satellite's science mission had come to an end in December 2010.

Due to the specific orbits, DEMETER was always located either shortly before the local noon (10:30 LT) or local midnight (22:30 LT) above the same point. The satellite performed 14 orbits per day and measured continuously between −65° and +65° of invariant latitude every 2 s in survey mode.

The major scientific objectives of the satellite were to study the ionospheric disturbances in relation to seismic activity and to examine the pre- and post-seismic effects (Parrot, 2002). The first paper, showing examples of unusual ionospheric observations made by the DEMETER satellite over seismically active regions, was published by Parrot et al. (2006a). Later, statistical investigations confirmed the existence of small but statistically significant decreases of wave intensity at a frequency around 1.7 kHz a few hours before an earthquake (Nemec et al., 2009; Píša et al., 2013).

DEMETER observations also provide a new possibility to analyze ground based transmitter signals that may be detected onboard the satellite above seismic regions. Such observations have been undertaken on many satellites for the investigation of VLF wave propagation and VLF wave interaction with ionospheric plasma (e.g. Aubrey, 1968; Inan and Helliwell, 1982). However, in the application of VLF signals to long-time seismic effects special data processing is necessary. Therefore, it can be considered as a new method of ionospheric sounding in association with seismicity. The first results of such analysis have been reported by Molchanov et al. (2006) for several strong earthquakes that occurred in 2004. The method estimated changes in the reception zone of the transmitters signal using the signal to noise ratio. An evident effect that occurred before and during the great Sumatran earthquakes with long-time duration of the order of one month has been confirmed later by Solovieva et al. (2009). After the first publication, similar effects were observed in the transmitter signals received onboard DEMETER during periods of strong seismic activity (e.g. Muto et al., 2008; Boudjada et al., 2008; Slominska et al., 2009; YuFei et al., 2009).

However, the method of reception zone changes does not allow for separating pre-seismic and post-seismic effects. Therefore a new method of satellite data processing has been developed

* Corresponding author.
*E-mail address:* rozhnoi@ifz.ru (A. Rozhnoi).

http://dx.doi.org/10.1016/j.pce.2015.02.005
1474-7065/

(residual method) which is similar to the data processing used at ground stations. In this work we summarize the results of a joint analysis of the satellite and ground-based measurements in connection with strong earthquakes which occurred during the DEMETER mission in the Far Eastern region.

## 2. Used data

### 2.1. Satellite data

The high-quality DEMETER database has been built during the mission. It includes data from several instruments which provided a nearly continuous survey of the plasma, waves and energetic particles. All details concerning the onboard experiments can be found in Berthelier et al. (2006a,b), Lebreton et al. (2006), Parrot et al. (2006b) and Sauvaud et al. (2006).

For our analysis we chose data recorded by the electric field receiver (ICE) for night orbits. Signals of the powerful VLF transmitters were clearly seen in the electric field data (Fig. 1). Frequency resolution of the spectra was $\Delta F = 19.5313$ Hz in the range of $F \leqslant 20$ kHz and it was worse ($\Delta F = 3.255$ kHz) at higher frequency range 3 kHz $\leqslant F \leqslant 3$ MHz, so that we mainly used the signals with $F \leqslant 20$ kHz for our analysis. In this frequency range the NWC transmitter signal (19.8 kHz) is the most powerful. The reception zone of this signal covers entirely all Eastern hemisphere (Rozhnoi et al., 2007b), and therefore we could analyze the signal in a large area including Japan and Kuril Islands.

The first step in satellite data processing was to obtain the intensity of the VLF transmitter signal. At this point it was necessary to correct the collected data for parasitic effects such as the instrument background noise and the natural emissions that can superimpose themselves on the signal. It was necessary, however, to take into account the influence of the scattering which was the major effect for some parts of the DEMETER orbit. Therefore as the main characteristic of a VLF/LF signals, we computed the signal to noise ratio (SNR) as follows:

$$\mathrm{SNR} = 2A(F_0)/[A(F_+) + A(F_-)] \quad (1)$$

where $A(F_0)$ is the amplitude of spectrum density for the frequency band that includes the transmitter frequency $F_0$. The amplitude $A$ ($F_0$) was estimated based on how well the transmitter frequency coincided with discrete frequency of the spectrum. This may be done using either the amplitude of the signal in the frequency band closest to $F_0$ or the average of the amplitudes of the two frequency channels that bracket $F_0$. $A(F_\pm)$ are the minimum amplitude values inside of the signal band ($\delta F$).

The choice of $F_\pm$ depended mainly on the transmitter power and position of the reception point. Usually $\delta F$ was 150–300 Hz, but for the powerful transmitters such as NWC (19.8 kHz) it could reach a value of 500 Hz when the satellite was in vicinity of the transmitter. As a result we produced a computation of $F_\pm$ for each VLF/LF signal and each selected orbit by a special procedure.

### 2.2. Ground-based data

Mainly data measured in VLF receiving station in Petropavlovsk–Kamchatsky (Russia) were used for the analysis. OmniPAL receiver was installed in Petropavlovsk–Kamchatsky (geographic coordinates; 53.090N, 158.550E) in June 2000 within the framework of Japanese-Russian ISTC project. The receiver in Kamchatka is a part of the Far East (or Pacific) network which has been formed after the installation of seven Japanese stations. All the stations receive simultaneously both the amplitude and phase of MSK (Minimum Shift Key) modulated signals from the same four transmitters: JJY (40 kHz, Fukushima) and JJI (22.2 kHz, Miyazaki) in Japan, NWC (19.8 kHz, Australia) and NPM (21.4 kHz, Hawaii). MSK signals have fixed frequencies in narrow band 50–100 Hz around the main frequency and adequate phase stability. The receivers can record signals with time resolutions ranging from 50 ms to 60 s. For our purpose we use sampling frequency of 20 s. The relative locations of the transmitters and two of our observing stations are plotted in Fig. 2. Among them the signals from JJY and JJI transmitters are most interesting for our analysis owing to the fortunate position of Petropavlovsk–Kamchatsky (PTK) station relative to the transmitters. The path NWC-PTK is somewhat outside the area of the main earthquakes in Japan and Kuril Islands, it is very long (about 10,000 km) and also crosses the equator where typhoon activity is very strong. Besides, the path passes through Indonesia, the region with strong seismic activity. So, this path is rather difficult for the ground analysis because the effects are cumulative.

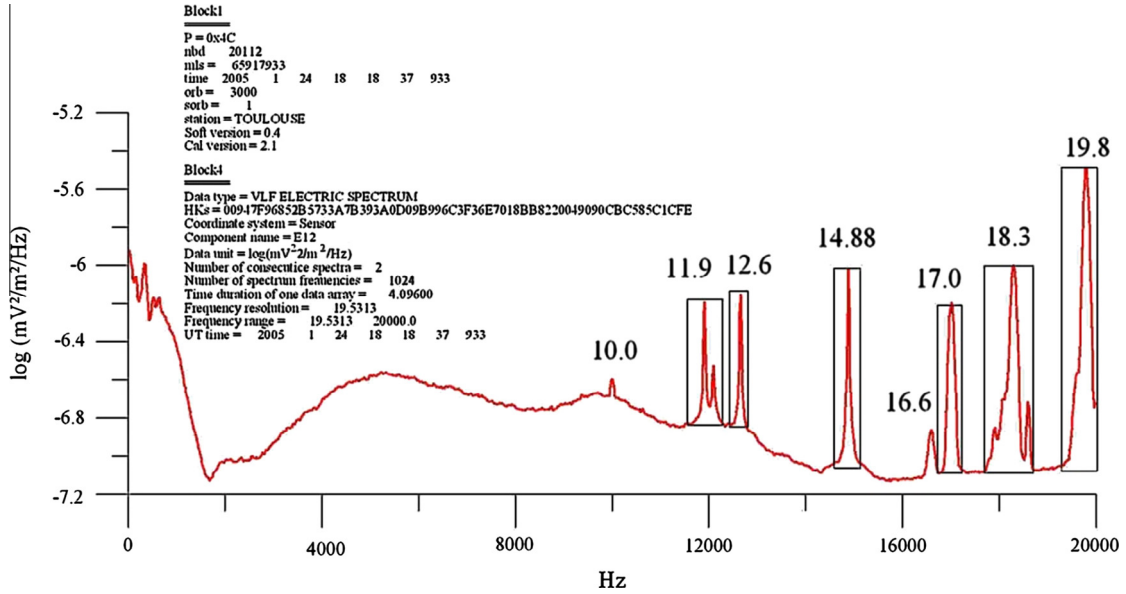


**Fig. 1.** An example of the summary spectrum for one night orbit recorded by ICE on board of the DEMETER (in frequency range 19.53 Hz-20 kHz). Signals of the several powerful VLF transmitters are easily noticed as vertical peaks in the dynamic spectra.

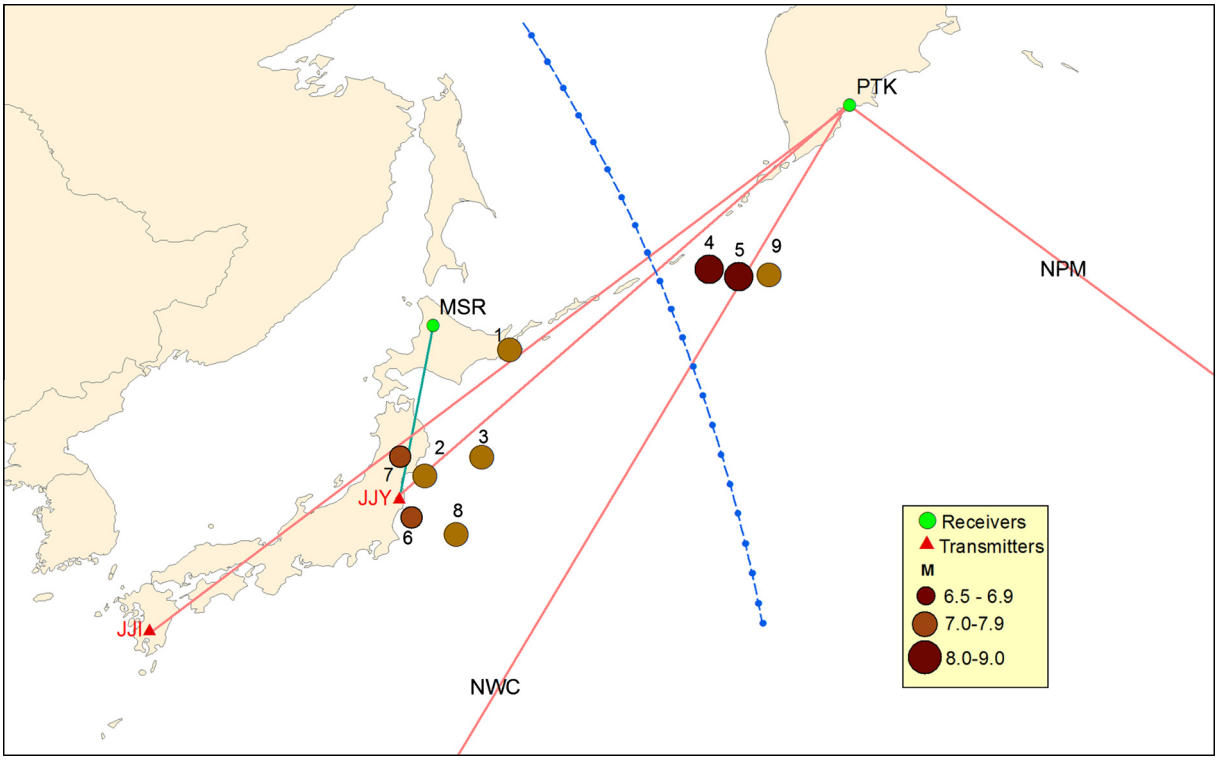


**Fig. 2.** A map showing the position of the stations in Petropavlovsk-Kamchatsky (PTK) and Moshiri (MSR) and the VLF/LF transmitters (JJI and JJY) together with the epicenter of the earthquakes under consideration. The directions to the NWC and NPM transmitters is indicated. An example of the part of a night orbit passing above the earthquake area is shown by blue line. (For interpretation of the references to color in this figure legend, the reader is referred to the web version of this article.)

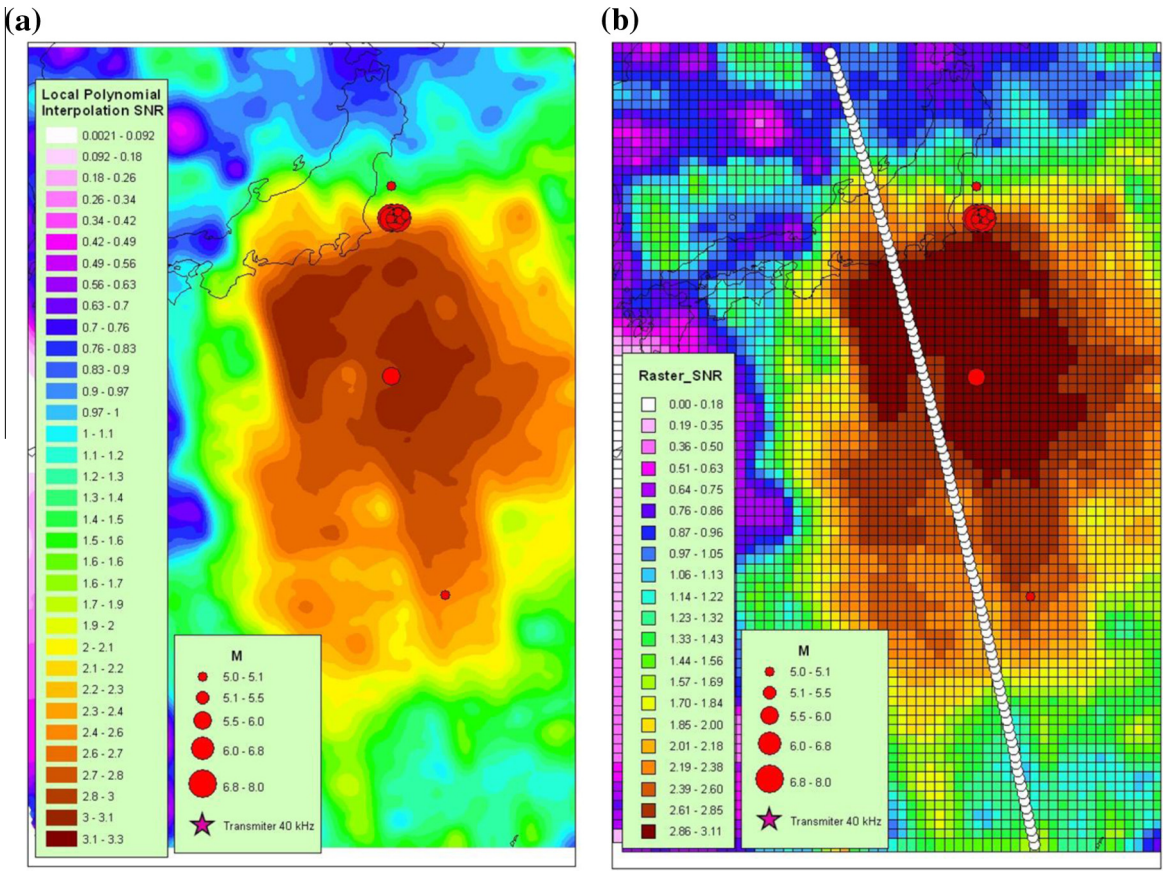


**Fig. 3.** (a) Example of a polynomial expression computing (for JJY signal). (b) Example of a net point model construction. White line shows the position of a real orbit.

Analysis was made for the earthquakes with their epicenters inside three Fresnel zones (the sensitivity zone). The semi-width ($y$) of the 1st Fresnel zone is:

$$y \approx [\lambda^2/4 + \lambda x(l - x/D)]1/2 \quad (2)$$

where $\lambda$ is the wavelength, $x$ is the coordinate along the path, and $D$ is the distance between transmitter and receiver.

## 3. Method of analysis

The day and nighttime ionosphere has different characteristics. Solar UV and X-ray radiation dominates the ionization processes during the day, so ionization is very significant. During the night, non-solar sources (e.g. cosmic rays, meteoric ionization, etc.) maintain the smaller free electrons and ions concentrations. Therefore

**Table 1**
Presence of anomalies in the VLF/LF transmitter signals before strong earthquakes in the Far East region during DEMETER mission.

| N | Date (d, m, y) | *M* | Depth, km | Presence of anomalies | | Comment |
|---|---|---|---|---|---|---|
| | | | | Ground | Satellite | |
| 1 | 28.11.2004 | 7.1 | 39 | + | + | |
| 2 | 16.08.2005 | 7.2 | 36 | + | + | |
| 3 | 14.11.2005 | 7.0 | 11 | + | | Missed data in the satellite |
| 4 | 15.11.2006 | 8.3 | 34 | + | + | |
| 5 | 13.01.2007 | 8.2 | 11 | ± | + | |
| 6 | 7.05.2008 | 6.8 | 35 | + | + | |
| 7 | 13.06.2008 | 6.9 | 10 | + | + | |
| 8 | 20.07.2008 | 7.0 | 22 | – | + | Outside sensitivity zone |
| 9 | 1.15.2009 | 7.4 | 36 | – | + | Outside sensitivity zone |

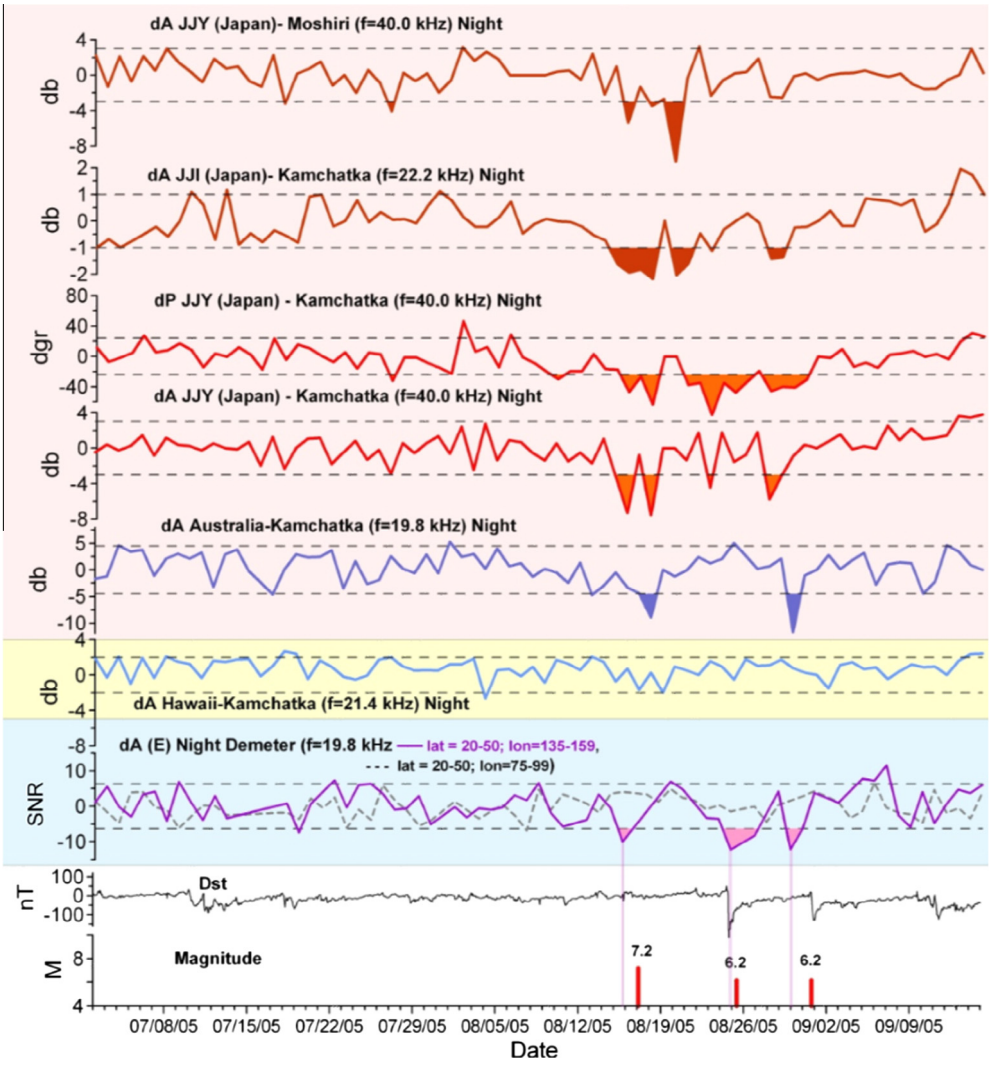


**Fig. 4.** Averaged through night residual VLF/LF signals in the ground observation for the wave paths: JJY-Moshiri, JJI-Kamchatka, JJY-Kamchatka, NWC-Kamchatka, and NPM-Kamchatka and residual satellite VLF signal observed on board of the DEMETER from the reception of NWC transmitter signal: solid line for the data above Japan, dash line - for the data aside of Japan area. Horizontal dotted lines show the $2\sigma$ level. Two panels below are Dst variations and earthquakes magnitude values.

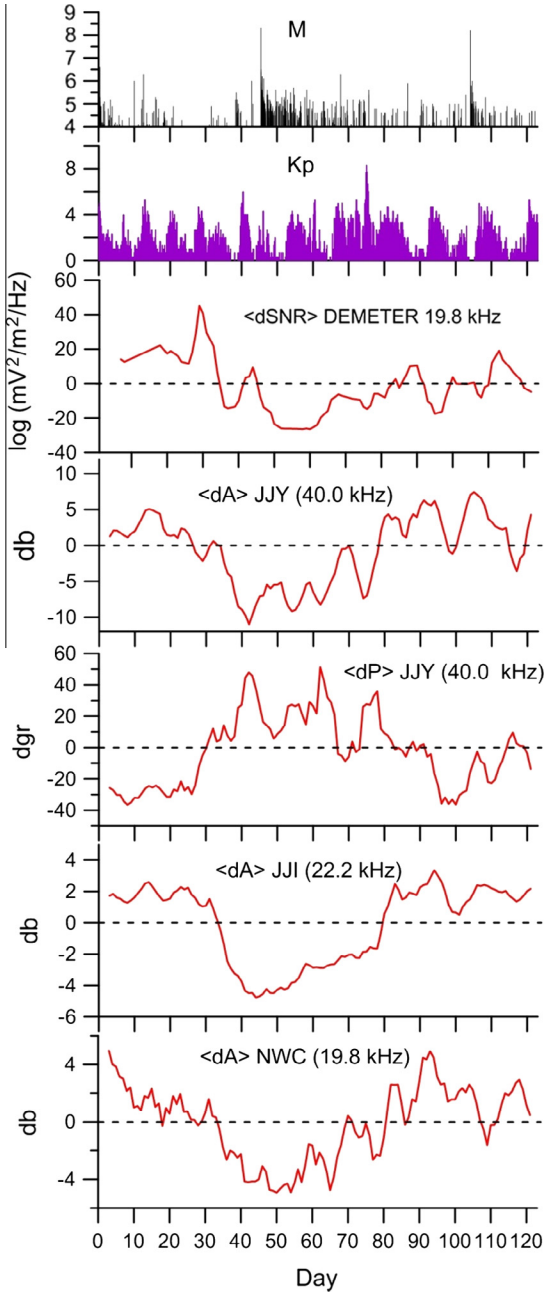


**Fig. 5.** Comparison of ground and satellite observations during October 2006 – January 2007. For the satellite observations averaged along part of the orbits VLF signal differences from the reception of NWC transmitter signal are shown. For ground observations averaged through night time VLF/LF signal differences are shown for the wave paths: JJY-Petropavlovsk-Kamchatsky (amplitude and phase), JJI-Petropavlovsk-Kamchatsky and NWC-Petropavlovsk-Kamchatsky. Axis *X* shows the days beginning from the 1st of October 2006. Two upper panels represent earthquake magnitude and Kp index of magnetic activity.

nighttime ionosphere is not such stable and provides optimal conditions for the detection of ionospheric disturbances (caused by magnetic storms, earthquakes, tsunami, etc.) by the VLF/LF signals. We therefore considered measurements only during nighttime both for the satellite and ground observations.

The ground and satellite data were processed by a method based on the difference between the real signal in nighttime and the model one (Rozhnoi et al., 2004). The model for the ground observation is based on monthly averaged signals calculated using data from quiet days. The models of the seasonal variation in the amplitude and phase of signals are used to remove the general trends in the data, leaving a residual signal of phase d$P$ or amplitude d$A$ which is defined as the difference between observed signal $P(t)$, $A(t)$ and model signal $\langle P\rangle$, $\langle A\rangle$:

$$dA(t) = A(t) - \langle A\rangle, \quad dP(t) = P(t) - \langle P\rangle \tag{3}$$

After that we calculated averaged through night residual signals.

For the satellite data we built a reference surface for SNR over the region of interest. To build the reference surface we used the method of local polynomial interpolation which provides a polynomial expression for the reference level as a function of longitude and latitude. The main problem in modeling was to interpolate irregular data into regular net. Local polynomial interpolation calculates predictions from the measured points within neighborhoods. The shape, maximum and minimum number of points to use, and the sector configuration can be specified. The weights of the sample points within the neighborhood decrease with distance. This technique predicts a value that is different from the measured value to avoid sharp peaks or depression in the output surface (details in Rozhnoi et al., 2012).

Model construction was performed using the Geo-Information System (GIS). GIS provides the tools for high-speed and accurate modeling and analysis of spatial information. Data for 3 months was used in order to remove any effects due to seasonal variations.

The modeling consists of the following procedure:

1. Computing a polynomial expression for the surface as a function of longitude and latitude (Fig. 3a).
2. Construction of the regular latitude and longitude grid 0.32°.
3. Computing of a net point model (Fig. 3b).

Using the reference surface, at any time and for any longitude and latitude in an active region, it is possible to define the variations of the VLF signal as the difference between the measured amplitude ($t$, longitude, latitude) and the reference value (longitude, latitude). For further analysis we used the averaged residual SNR along the part of orbit passing above region under investigation. The longitudinal width of the analyzed zone was 25° that provided one orbit for every day. The position of zone was different depending on the position of the epicenters of earthquakes. An example of the part orbit passing above seismic area can be seen in Fig. 2.

## 4. Results of joint analysis

The method of residual signal was applied for the joint satellite and ground-based analysis of VLF/LF transmitter signals for the periods of strong ($M \geqslant 6.8$) seismic activity near Japan and in Kuril Islands region. Nine such earthquakes (catalogue USGS) occurred in that area during DEMETER mission (2004–2010). The information about the earthquakes can be found in Table 1. Below we provide details for every event.

1. Earthquakes in November–December 2004.

The period of analysis was from 1 October 2004 to 24 January 2005. This period had a very quiet seismic regime until November and rather strong seismic activity in November and December 2004 in the North Japan and North Kuril Islands. Seismic activity inside the sensitivity zone of JJY-PTK path was determined by three series of earthquakes ($M$ = 5.6–7.1) and three series of the negative anomalies in the phase and amplitude of the LF signal were observed several days before and after the earthquakes. This case was thorough investigated in the works (Rozhnoi et al., 2006, 2007b). Unfortunately, there was a gap in the DEMETER data in October and December that reduced the reliability of the satellite

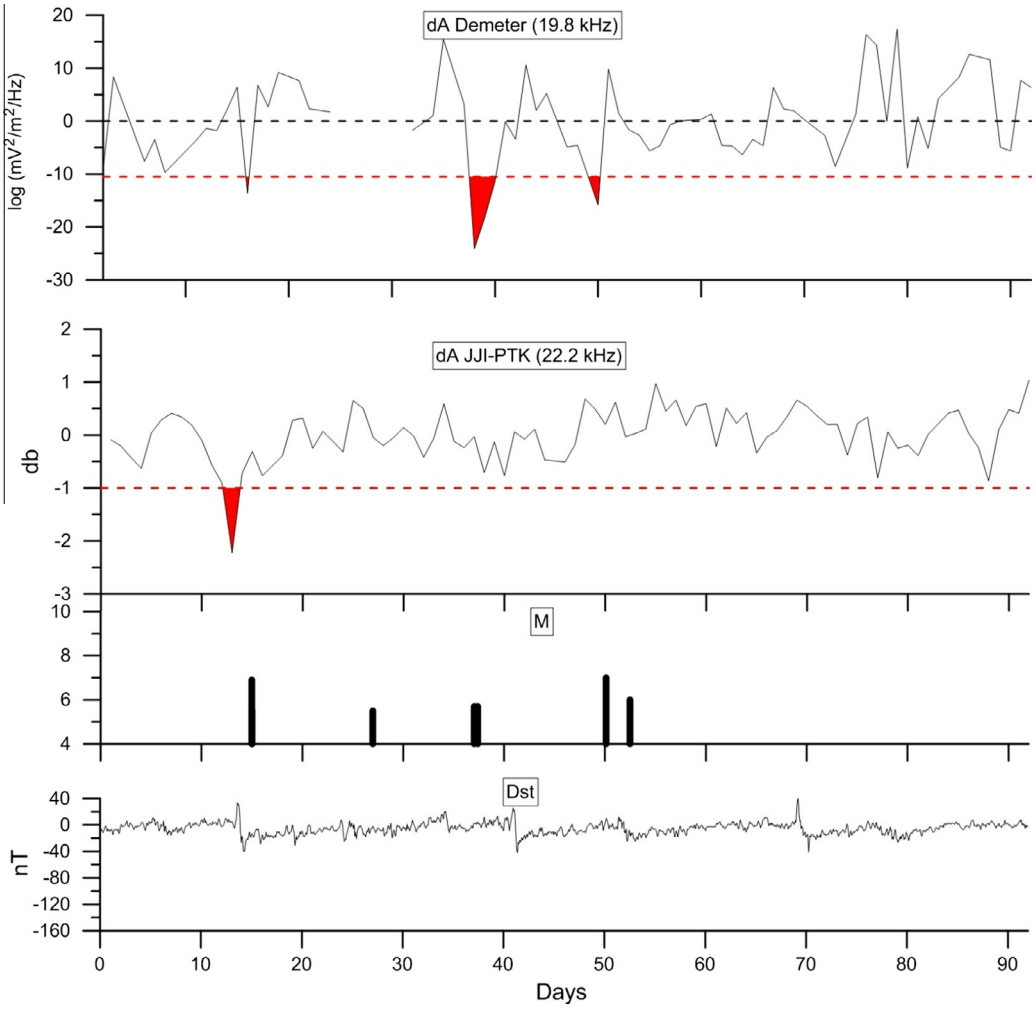


**Fig. 6.** Satellite and ground observations during June–August 2008. For the satellite observations averaged along part of the orbits VLF signal differences from the reception of NWC transmitter signal are shown. For ground observations averaged through night time VLF signal differences are shown for the wave paths JJI-PTK. Axis *X* shows the days beginning from the 1st of June 2006. Red dotted lines show the $2\sigma$ level. Two bottom panels represent earthquake magnitude and Dst index of magnetic activity. (For interpretation of the references to color in this figure legend, the reader is referred to the web version of this article.)

observations, although an anomalous decrease in the DEMETER data was also found before the strongest earthquake in November ($M = 7.1$).

2. Seismic activity near Japan in August 2005.

The earthquake with $M = 7.2$ took place on 16 August 2005 off the coast of the Island Honshu. After that, during two weeks, there were several earthquakes with $M \sim 6$ at the same region. The epicenters of earthquakes were inside the sensitivity zones of paths: JJY-PTK, JJI-PTK and JJY-Moshiri and very close to the path of NWC-PTK (Fig. 2). The DEMETER data from NWC transmitter has been analyzed both above Japan and above a control area that was situated at the same latitudes and has approximately the same level of the signal, but without earthquakes in the period under consideration. A comparison of ground-based and satellite data for the period July–September is shown in Fig. 4. Six upper panels show averaged through night residual signals in the ground observation while the next panel shows averaged satellite residual signal observed on board of the DEMETER both in the area above Japan (solid line) and in the control area (dash line). Two panels below are Dst variations and earthquakes magnitude values.

Negative anomalies in the signals are clearly seen in all the ground paths beside the path NPM-PTK, which was a control path. The type of anomalies is somewhat different. The anomalies from two Japanese transmitters appear two days before the first earthquake ($M = 7.2$) and last until the end of seismic activity. Among them the decrease of the phase of JJY signal is the most prominent. Anomalies of the amplitude from the NWC transmitter are not so clear. Results of the satellite observation are in a good agreement with ground data, and a significant decrease of SNR values above Japan is observed in 2–3 days before every earthquake.

3. The earthquake on 14 November 2005.

The earthquake with $M = 7.0$ occurred on 14 November 2005 to the east of Honshu Island. This case was considered for ground-based data by Rozhnoi et al. (2007a). The disturbances in amplitude and phase of JJY signal recorded in PTK station were observed during approximately two weeks before the earthquake. Unfortunately, the DAMETER data for this period is absent.

4 and 5. The Simushir earthquakes on 15 November 15 2006 and 13 January 2007 (Kuril Islands).

The very strong earthquake with $M = 8.3$ took place near the Simushir island of the Central Kuril region (Russia) on 15 November 2006. Following this, a series of strong aftershocks ($M = 5$–$6.5$)

observed during several months. After that the second strong earthquake ($M$ = 8.2) occurred approximately in the same area on 13 January 2007. The earthquake's epicenter was in the sensitivity zone of wave paths JJY-PTK, JJI-PTK and NWC-PTK. The detailed analysis of anomalies observed in the period from 1 October 2006 to the end of January 2007 both in ground and satellite data was made by Rozhnoi et al. (2012). Here we give only the final result of the joint analysis. Fig. 5 presents a comparison of the results of both satellite and ground observations. The top panel shows the magnitude of earthquakes and aftershocks that occur within the seismic region during the period of interest. The second panel shows the interplanetary Kp index. The third panel shows the residual satellite signal amplitude (dSNR) when compared to the model signal representing the expected signal variation during undisturbed periods. The lower four panels show the residual amplitude (d$A$) and phase (d$P$) of the transmitter signals as recorded by the receiver PTK. There is an evident decrease in the amplitude of VLF/LF signals both in the ground and in the satellite data in association with seismicity. The amplitude anomalies are always negative. This signature can result from the effects of magnetic storms, seismic activity, tsunami propagation, volcano eruptions, change of atmospheric pressure (e.g. during typhoons) etc. and it is due to the losses of the signal in the ionosphere irregularities during propagation. Phase anomalies can be both positive and negative. It depends on the length of the path. The reflection altitude of the ionosphere changes when irregularities appear which leads to the change of the signal propagation length. So, the difference in phase between a receiver and transmitter can shift on either side. In the present case, the anomalies in the phase of the JJY signal are positive.

Unlike the previous case, both the satellite and ground anomalies were observed for a very long time. They appeared about a fortnight before the earthquake and lasted until the middle of December.

Regarding the second Simushir earthquakes on 13 January 2007, it was a little outside the sensitivity zones for the JJY-PTK and JJI-PTK paths and small anomalies in the NWC signal were seen only in the DEMETER data several days before the earthquake. Disturbances in JJY signal was recorded in the ground data on 7–8 January, but these disturbances were not significant in comparison with the very strong anomalies observed before and after the first earthquake. Long and rather strong anomalies both in the satellite and ground data clearly seen during a month after the earthquake were most likely induced by the post-seismic relaxation. However, they can also be the pre-seismic effect of the second earthquake. In the present case we cannot, with certainty, separate pre- and post-seismic effects.

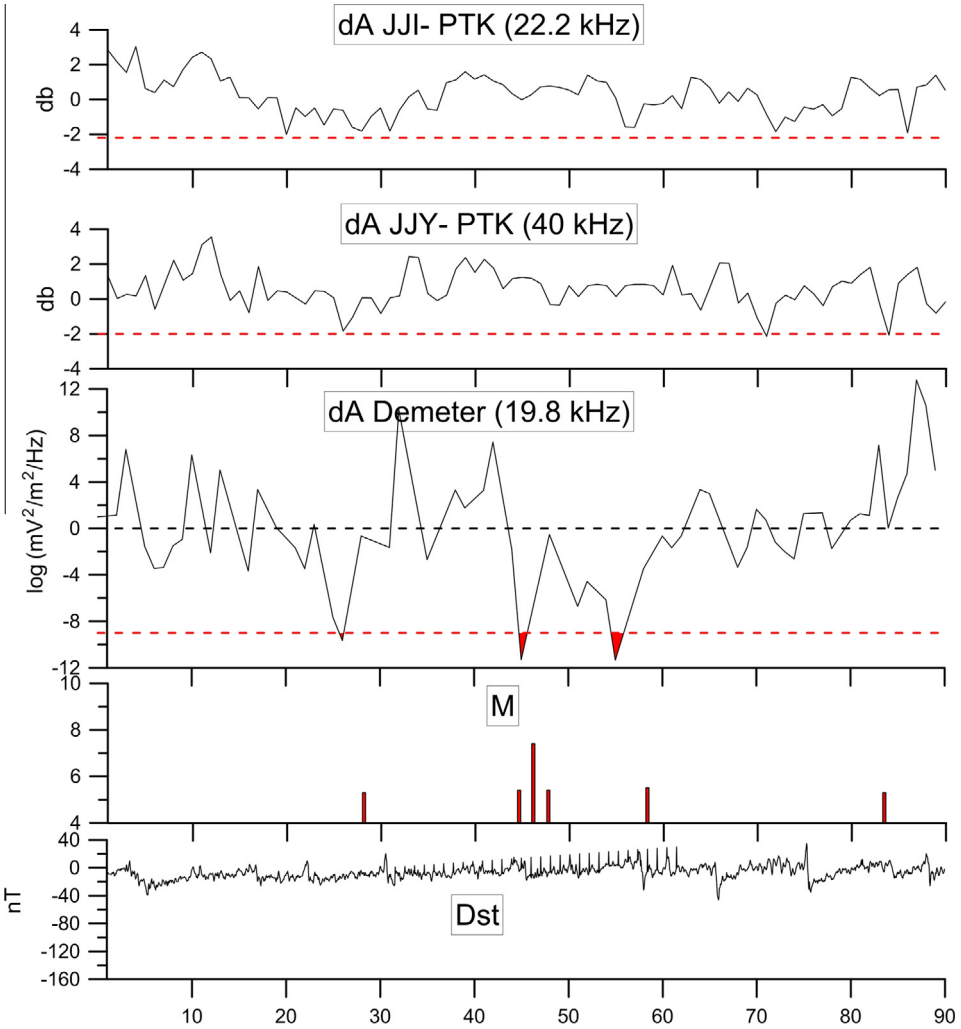


**Fig. 7.** Ground and satellite observations during December 2008 – February 2009. Averaged over night signals (JJI and JJY) for ground observations are shown. For satellite data averaged along part of the orbits VLF signal differences from the reception of NWC transmitter signal are shown. Axis $X$ shows the days beginning from the 1st of December 2008. Red dotted lines show the $2\sigma$ level. Two bottom panels represent earthquake magnitude and Dst index of magnetic activity. (For interpretation of the references to color in this figure legend, the reader is referred to the web version of this article.)

6. The earthquake in the north part of Honshu Island (Japan) on 7 May 2008 ($M = 6.8$).

In the analysis of this earthquake (unlike all the other cases) the signal of the JJY (40 kHz) transmitter was used both for the DEMETER and ground observations (Rozhnoi et al., 2010). It was possible to do this because the epicenter of the earthquake was located in the maximum signal reception zone for satellite data (which is rather local and covers a small area with radius about 1000 km). The signal was analyzed above the seismic active region and in the magnetically conjugate area. A signal from the JJI (22.2 kHz) transmitter was additionally used in ground observations.

The period of analysis was from April 18 to June 27. Strong foreshock activity preceded the earthquake. It began on 5 May and two of the strongest foreshocks ($M = 6.2$ and $M = 6.1$) occurred shortly before the main shock. After the earthquake there were a series of aftershocks with the strongest ($M = 5.6$) on the next day.

Results of ground data analysis revealed a clear decrease during several days before the earthquake both in the JJI and in JJY signals. The decrease of the signals began 5 days before the earthquake and had the maximal drop 3 days before the earthquake. The effect is more evident for the amplitude and phase of JJY signal. In the phase there was also a noticeable effect 5–6 days after the earthquake.

For the satellite observation it was found that there was an enhancement of the signal before and after the earthquake in the area above the seismic active region (North). An increase of the residual SNR started 3 days before the earthquake, reached maximum the next day after the earthquake, and continued 3 days after it. In the magnetically conjugate area (South) the situation was quite the opposite. Depletion in the signal was observed in the period of its enhancement in the Northern area. Anomalies in satellite data precisely coincided in time with those in the ground-based data. The mechanism of observed effects, able to produce the opposite behavior of SNR in South and North, cannot be defined. At this purpose, more data and other information must be collected.

It should be noted that during all the period of analysis (April-June 2008), no signal anomalies in the control paths have been observed and there was rather weak magnetic activity.

7 and 8. Seismic activity in June-July 2008 in the Honshu region of Japan.

Data from NWC transmitter received by the DEMETER satellite and data from JJI transmitter received in PTK station was used for the analysis. The period of analysis was from the 1 June to the end of August. Two strong earthquakes occurred during this period. The first earthquake with a magnitude 6.9 took place on June 13, 2008 and the second earthquake with $M = 7.0$ happened on July 20, 2008. The epicenter of the first earthquake was within the sensitivity zone of the propagation path JJI-PTK while the epicenter of the second earthquake was outside the sensitivity zones for any path for ground observations. The results of the satellite and ground observations are presented in Fig. 6. It is clearly seen that there is a decrease in the observed signals during the period 1–2 days before the first earthquake both for satellite and ground data. Such a lead time of a few days (up to a week or so) is comparable to the time from the approach of the system to the critical point (Sarlis et al., 2010; Varotsos et al., 2011) until the main shock occurrence as identified by the natural time analysis of seismicity subsequent to Seismic Signals Activity (Varotsos et al., 2008, 2009). For the following earthquakes the effect is observed only for satellite data.

9. The earthquake on 15 January 2009 in the Central Kuril Islands region.

During the period from the beginning of December 2008 until the end of February 2009 several earthquakes ($M = 5.3$–$7.4$) occurred in the Kuril–Kamchatka region. The strongest earthquake was recorded on January 15 and had a magnitude of 7.4. The epicenters of all the earthquakes were outside the sensitivity zone for the propagation path from the transmitter JJY to the receiver in PTK. The signal in this path was undisturbed during the period of analysis (Fig. 7 second panel). Some weak earthquakes were within the path JJI–PTK but the signal is unaffected as it is seen from Fig. 7 (upper panel). The third panel in Fig. 7 shows the residual SNR for DEMETER data (NWC transmitter). The next panel shows the onset times of the earthquakes during the period of analysis. The lower panel shows the Dst geomagnetic index. As can be seen from the third panel, there are three large decreases in the amplitudes of the electric field which are observed. Each decrease occurs 2–3 days before the onset of an earthquake.

## 5. Conclusion and discussion

The results of the joint satellite and ground-based analysis of the VLF/LF transmitter signals during DEMETER mission are presented in Table 1.

A comparison of ground and satellite observations of VLF/LF signal from ground transmitters demonstrates good coincidence results. For satellite observations anomalies in the signals have been found for all the earthquakes where full data were available. For ground observations, anomalies were observed if the epicenters of earthquakes were inside sensitivity zones of wave propagation paths. The character (duration, time of appearance) of anomalies was very close in satellite and ground data depending on every specific earthquake. Such simultaneous analysis provides a cross validation of the observations and hence a higher reliability in the results.

## Conflict of interest

There is no conflict of interest.

## Acknowledgements

This research is supported by Royal Society International Exchanges Scheme and RFBR under Grant 13-05-92602 KOa.

## References

Aubrey, M.P., 1968. Six-component observation of VLF signal on FR-1 satellite. J. Atmos. Terr. Phys. 30, 1161–1169.
Berthelier, J.J., Godefroy, M., Leblanc, F., Seran, E., Peschard, D., Gilbert, P., Artru, J., 2006a. IAP, the thermal plasma analyzer on DEMETER. Planet. Space Sci. 54 (5), 487–501.
Berthelier, J.J., Godefroy, M., Leblanc, F., Malingre, M., Menvielle, M., Lagoutte, D., Brochot, J.Y., Colin, F., Elie, F., Legendre, C., Zamora, P., Benoist, D., Chapuis, Y., Artru, J., 2006b. ICE, the electric field experiment on DEMETER. Planet. Space Sci. 54 (5), 456–471.
Boudjada, M.Y., Schwingenschuh, K., Biernat, H.K., Berthelier, J.J., Blecki, J., Parrot, M., Stachel, M., Aydogar, O., Stangl, G., Weingrill, E., 2008. Similar behaviors of natural ELF/VLF ionospheric emissions and transmitter signals over seismic Adriatic regions. Nat. Hazards Earth Syst. Sci. 8, 1229–1236.
Cussac, T., Clair, M.A., Ultré-Guerard, P., Buisson, F., Lassalle-Balier, G., Ledu, M., Elisabelar, C., Passot, X., Rey, N., 2006. The DEMETER microsatellite and ground segment. Planet. Space Sci. 54 (5), 413–427.
Inan, U.S., Helliwell, R.A., 1982. DE-1 observations of VLF transmitter signals and wave-particle interaction in the magnetosphere. Geophys. Res. Lett. 9, 917–923.
Lebreton, J.P., Stverak, S., Travnicek, P., Maksimovic, M., Klinge, D., Merikallio, S., Lagoutte, D., Poirier, B., Kozacek, Z., Salaquarda, M., 2006. The ISL Langmuir Probe experiment and its data processing onboard DEMETER: scientific objectives, description and first results. Planet. Space Sci. 54 (5), 472–486.
Molchanov, O.A., Rozhnoi, A., Solovieva, M., Akentieva, O., Berthelier, J.-J., Parrot, M., Lefeuvre, F., Biagi, P.-F., Castellana, L., Hayakawa, M., 2006. Global diagnostics of ionospheric perturbations associated with seismicity using VLF transmitter signals received on DEMETER satellite. Nat. Hazard Earth Syst. Sci. 6, 745–753.

Muto, F., Yoshida, M., Horie, T., Hayakawa, M., Parrot, M., Molchanov, O.A., 2008. Detection of ionospheric perturbations associated with Japanese earthquakes on the basis of reception of LF transmitter signals on the satellite DEMETER. Nat. Hazards Earth Syst. Sci. 8, 135–141.

Nemec, F., Santolík, O., Parrot, M., 2009. Decrease of intensity of ELF/VLF waves observed in the upper ionosphere close to earthquakes: a statistical study. J. Geophys. Res. 114, A04303. http://dx.doi.org/10.1029/2008JA01397.

Parrot, M., 2002. The micro-satellite DEMETER: data registration and data processing. In: Hayakawa, M., Molchanov O. Terrapub. (Eds.), Seismo Electromagnetics: Lithosphere-Atmosphere-Ionosphere Coupling, pp. 660–670.

Parrot, M., Berthelier, J.J., Lebreton, J.P., Sauvaud, J.A., Santolik, O., Blecki, J., 2006a. Examples of unusual ionosperic observations made by the DEMETER satellite over seismic regions. Phys. Chem. Earth 31 (4–9), 486–495.

Parrot, M., Benoist, D., Berthelier, J.J., Blecki, J., Chapuis, Y., Colin, F., Elie, F., Fergeau, P., Lagoutte, D., Lefeuvre, F., Legendre, C., Lévêque, M., Pinçon, J.L., Poirier, B., Seran, H.C., Zamora, P., 2006b. The magnetic field experiment IMSC and its data processing onboard DEMETER: scientific objectives, description and first results. Planet. Space Sci. 54 (5), 441–455.

Píša, David, Němec, František, Santolík, Ondřej, Parrot, Michel, Rycroft, Michael, 2013. Additional attenuation of natural VLF electromagnetic waves observed by the DEMETER spacecraft resulting from preseismic activity. J. Geophys. Res.: Space Phys. 118 (8), 5286–5295. http://dx.doi.org/10.1002/jgra.50469.

Rozhnoi, A., Solovieva, M.S., Molchanov, O.A., Hayakawa, M., 2004. Middle latitude LF (40 kHz) phase variations associated with earthquakes for quiet and disturbed geomagnetic conditions. Phys. Chem. Earth 29, 589–598.

Rozhnoi, A.A., Solovieva, M.S., Molchanov, O.A., Chebrov, V., Voropaev, V., Hayakawa, M., Maekawa, S., Biagi, P.F., 2006. Preseismic anomaly of LF signal on the wave path Japan-Kamchatka during November – December 2004. Phys. Chem. Earth 31, 422–427.

Rozhnoi, A., Solovieva, M., Molchanov, O., Biagi, P.-F., Hayakawa, M., 2007a. Observation evidences of atmospheric Gravity Waves induced by seismic activity from analysis of subionospheric LF signal spectra. Nat. Hazard Earth Syst. Sci. 7, 625–628.

Rozhnoi, A., Molchanov, O., Solovieva, M., Gladyshev, V., Akentieva, O., Berthelier, J.-J., Parrot, M., Lefeuvre, F., Hayakawa, M., Castellana, L., Biagi, P.F., 2007b. Possible seismo-ionosphere perturbations revealed by VLF signals collected on ground and on a satellite. Nat. Hazard Earth Syst. Sci. 7, 617–624.

Rozhnoi, A., Solovieva, M., Molchanov, O., Biagi, P.-F., Hayakawa, M., Schwingenschuh, K., Boudjada, M., Parrot, M., 2010. Variations of VLF/LF signals observed on the ground and satellite during a seismic activity in Japan region in May–June, 2008. Nat. Hazard Earth Syst. Sci. 10, 529–534.

Rozhnoi, Alexander, Solovieva, Maria, Parrot, Michel, Hayakawa, Masashi, Biagi, Pier Francesco, Schwingenschuh, Konrad, 2012. Ionospheric turbulence from ground-based and satellite VLF/LF transmitter signal observations for the Simushir earthquake (November 15, 2006). Ann. Geophys. 55 (1), 187–192. http://dx.doi.org/10.4401/ag-5190.

Sarlis, N.V., Skordas, E.S., Varotsos, P.A., 2010. Nonextensivity and natural time: the case of seismicity. Phys. Rev. E 82, 021110, http://dx.doi.org/10.1103/PhysRevE.82.021110.

Sauvaud, J.A., Moreau, T., Maggiolo, R., Treilhou, J.-P., Jacquey, C., Cros, A., Coutelier, J., Rouzaud, J., Penou, E., Gangloff, M., 2006. High-energy electron detection onboard DEMETER: The IDP spectrometer, description and first results on the inner belt. Planet. Space Sci. 54, 502–511.

Slominska, E., Blecki, J., Parrot, M., Slominski, J., 2009. Satellite study of VLF ground-based transmitter signals during seismic activity in Honshu Island. Phys. Chem. Earth 34, 464–473. http://dx.doi.org/10.1016/j.pce.2008.06.016.

Solovieva, M.S., Rozhnoi, A.A., Molchanov, O.A., 2009. Variations in the parameters of VLF signals on the DEMETER satellite during the periods of seismic activity. Geomag. Aeron. 49 (4), 532–541.

Varotsos, P.A., Sarlis, N.V., Skordas, E.S., Lazaridou, M.S., 2008. Fluctuations, under time reversal, of the natural time and the entropy distinguish similar looking electric signals of different dynamics. J. Appl. Phys. 103, 014906. http://dx.doi.org/10.1063/1.2827363.

Varotsos, P.A., Sarlis, N.V., Skordas, E.S., 2009. Detrended fluctuation analysis of the magnetic and electric field variations that precede rupture. CHAOS 19, 023114. http://dx.doi.org/10.1063/1.3130931.

Varotsos, Panayiotis, Sarlis, Nicholas V., Skordas, Efthimios S., Uyeda, Seiya, Kamogawa, Masashi, 2011. Natural time analysis of critical phenomena. PNAS 108 (28), 11361–11364. http://dx.doi.org/10.1073/pnas.1108138108.

YuFei, He, DongMei, Yang, HuaRan, Chen, JiaDong, Qian, Rong, Zhu, Parrot, M., 2009. SNR changes of VLF radio signals detected onboard the DEMETER satellite and their possible relationship to the Wenchuan earthquake. Sci. China, Ser. D Earth Sci. 52 (6), 754–763. http://dx.doi.org/10.1007/s11430-009-0064-5.